TD-2 | 231

ASAT

MILITARY TECHNICAL COLLEGE
CAIRO - EGYPT

TURBULENT VELOCITY OF REACTION

Elkotb,M.M, Salem,H and Abou-Arab,T.W[1]

Faculty of Engineering, Cairo University
EGYPT

ABSTRACT

Confined turbulent swirling combustion data obtained from gas chromatograph, gas analyzers, thermocouples and hot wire anemometer for a wide range of operating conditions are analyzed numerically. The effect of swirling flow, inlet velocity and equivalence ratio on different parameters with and without secondary air are discussed and analyzed. The obtained experimental data facilitated better and deep understanding of complicated problems associated with swirl reacting flow and provided in the same time generalized relations for the turbulent viscosity and velocity of chemical reaction required for the development of numerical prediction methods.

INTRODUCTION

Recent investigations of the factors affecting the performance of continuous flow combustion devices [1-4] have shown that coupling between fluid dynamic and chemical processes is a major factor in governing energy release and pollutants formation. The present understanding of the nature of this coupling is insufficient to allow quantitative prediction of the effect of changes in the operating conditions on combustor performance. However, analytical studies of turbulent reacting flows [5-8], using empirical relation for turbulent burning velocity, have provided some insight into the effects of mixing and turbulence on flow field structure and species concentration. It is known that the laminar burning velocity is physichemical constant that depends on mixture composition, temperature and pressure, and the turbulent burning velocity, which is not easy measured, depends also on the aerodynamic parameters. Some investigators [9-10] have measured and correlated the turbulent burning velocity with aerodynamic parameters in simplified systems for analytical models. Often in prctical combustors the problem is aggravated by hetrogenity of both composition and turbulence and diffusion as well as mixing

1. Currently Jordan University of Science and Technology. IRBID - JORDAN

which play an important role. This necessitates that the turbulent burning velocity has to be measured under practical combustor conditions. Moreover, detailed measurements in turbulent reacting flows are required to assess the validity of the present analytical combustor models. Few detailed measurements of temperature and species concentrations have been carried out on combustor models at various operating conditions [11-16] but these combustors were small and of complicated geometry. Also liquid fuels had been used and the conditions were complicated by fuel atomization and vaporation and no correlations of the turbulent burning velocity have been obtained.

In the present investigation, detailed measurements of temperature, species concentration and velocity have been carried out in a two dimensional swirl combustor fuelled with natural gas under variable operating conditions. The measurements have been used to calculate the effective turbulent burning velocity under wide ranges of operating conditions. These experimental data provide additional insight into the interaction between fluid dynamic and chemical processes in inturbulent diffusion flames and assessement of analytical turbulent reacting flow models.

APPARATUS AND PROCEDURE

A schematic of the opparatus used in the present study is shown in Fig.1. The combustor consists of a 120 mm diameter and 927 mm long flame tube with two conical ends. The length to diameter ratio is sufficient to provide flame stabilization, combustion and dilution. The combuster liner has 24 slots for secondary air admission arranged in 3 rings with 8 slots each to satisfy better stabitity and a nearly two dimensional flow in the combustor. The slots are 25.5 mm wide and 101.5 mm long. The secondary air flows in the annular space between the flame tube and the 300 mm diameter outer casing. The flame tube has tappings at 7 axial stations to fit probes for velocity and temperature measurements as well as for combustion products sampling. It is equipped with a hot wire anemometer x-type probe to measure the air velocity components [17].

At one of the conical ends a gas burner is attached, which consists of a central 9.5 mm internal diameter tube for fuel admission while the combustion air flows through an outer concentric tube of 52.2 mm diameter, then through a vane type swirler with different Vane angles 0-70° attached at the burner exit. The natural gas, which is composed of 82.76% methane, 8.17% ethane and traces of other gases, has been supplied at a regulated pressure of 5.2 bar then metered by a standard orifice meter. Air is supplied from a high pressure compressor at 8 bar and then devided to primary and secondary air before being fed to the combustor. Both secondary and primary air flow rates are measured by standard orifice meter.

6

Gas samples are withdrawn from different locations by water cooled stainless steel isokinetic probe. To ovoid quenching effect of the probe, uncooled cenvergent-divergent nozzle probe tip of throat diameter 0.4 mm has been used. The gas samples are conditioned and analyzed for CO, CO_2, O_2 and unburned hydrocarbons. Perkin Elmer model 3920 gas chromatograph coupled to a microcomputer has been used for measuring the concentration for most species and gaseous fuel. Paramagnetic analyser has been used to determine the oxygen concentration. In some runs, CO and CO_2 concentrations have been measured by NDIR gas analyzer while a flame ionzation detector has been used to measure the concentration of total unburned hydrocarbons.

The gas temperature at different locatians has been measured using type B (Pt+6%Rh versus pt+30%Rh) shielded thermocouples. The output of the thermocouples has been displayed on a digital simulator and the temperature is determined with an accuracy better than ±0.5%.

During experiments the inlet fuel velocity has been varied between 6 and 11 m/s and at each velocity the air flow rate has been adjusted to vary the overall equivalence ratio between 0.42 and 1.0. This has been carried out with and without secondary air admission.

TURBULENT VELOCITY OF REACTION

Swirl has large scale effets on turbulent flows and therefore size, shape, stability and combustion intensity are affected by the degree of swirl. The mean and turbulence characteristics of the swirling flow generated in gas turbine combustors are generally affected by the way of creating the swirl. The turbulence model, using either simple turbulent viscosity or differential turbulent viscosity expressions, simulates the behaviour of swirling flow in combustors. The value of the turbulent velocity of reaction depends to a great extent upon the used turbulence model. The present work deduces its value when using the two-equation turbulence model in the case of recirculating swirling flows.

The two-equation turbulence model solves differential equations for the turbulence kinetic energy k and its dissipation rate $\epsilon = C_D k^{3/2}/l$. From these, the turbulent viscosity, $\mu_t = C_D\, k^{1/2} l$, can be specified if the double velocity correlation $\overline{u_i' u_j'}$ are related to the Boussinesq eddy viscosity. They can be written in the polar coordinates for axisymmetric non isotropic in the following form:

$$-\rho\overline{u'^2} = 2\mu_{xx}\,\partial u/\partial x - (2/3)\rho k$$

$$-\rho\overline{v'^2} = 2\mu_{rr}\,\partial v/\partial r - (2/3)\rho k$$

$$-\rho\overline{w'^2} = 2\mu_{\theta\theta}\, v/r - (2/3)\rho k \qquad (1)$$

$$-\rho\overline{u'v'} = \mu_{rx}(\partial u/\partial r + \partial v/\partial x)$$

$$-\rho\overline{u'w'} = \mu_{x\theta}(\partial w/\partial x)$$

$$-\rho\overline{v'w'} = \mu_{r\theta} r\,\partial(w/r)/\partial r \qquad (2)$$

Velocity gradients are calculated from experimental time mean Velocities at different swirl ratios and sections downstream using a suitable finite difference technique and relating these to appropriate measurements of Reynolds stresses to deduce the turbulent viscocity components. A sample of experimental resuts is shown in Fig.2 with full details given elsewhere [17]. Using an optimization procedure optimal value of C_μ has been deduced in the following form:

$$C_\mu = 0.11\ (r/R)^{-0.08} \times (\theta/\theta_o)^{-0.88} \qquad (3)$$

For scaler fluxes (e.g. v'c') the following relations is adopted

$$-\overline{v'C'} = D_t\,\partial\overline{C}/\partial r \qquad (4)$$

where $D_t = \nu_t/\sigma_c$

Analyzing the diffusion process of fuel before burning it is found to depend to a great extent upon the burning temperature as a result of the mutual heat transfer and heat generation processes. Therefore, for generalization of results the combustion zone has been divided into two zones: the combustion zone at the flame front, characterized by maximum gradients of concentrations and velocities, and the zone downstream the flame front. The diffusion equations for an isothermal combustion process with two source components can be written in the following form:

$$v\,\partial C_f/\partial r + u\,\partial C_f/\partial x = D_t\nabla^2 C_f$$

$$v\,\partial C_o/\partial r + u\,\partial C_o/\partial x = D_t\nabla^2 C_o \qquad (5)$$

Splitting each variable to its mean and fluctuating values, utilizing the average principles, making the necessary boundary layer approximation and using Eq.4 the diffusion equations can be transformed to the following form:

$$u\,\partial C_f/\partial z = [D_t(1/r.\partial\overline{C}_f/\partial r + \partial^2\overline{C}_f/\partial r^2) + D_t(1/r\,\partial\overline{C}_f/\partial r + \partial^2 C_f/\partial r^2) - k_{\phi f}(\overline{C}_f, \overline{C}_o)$$

$$u\,\partial\overline{C}_o/\partial z = [D_t(1/r.\partial\overline{C}_o/\partial r + \partial^2\overline{C}_o/\partial r^2) + D_t(1/r.\partial\overline{C}_o/\partial r + \partial^2\overline{C}_o/\partial r^2)] - k_{\phi o}(\overline{C}_f, \overline{C}_o) \qquad (6)$$

6

The simultaneous solution of these partial differential equations has been carried out by averaging method if the distribution function of velocity and concentration at a given section is predetermined experimentally and transforming into ordinary differential equations. The dependence function of the source terms have been approximated and substituted in the elementary volume at any position as follows:

$$\pi R^2 \, ud\overline{C} = 2\pi R(D_{eff}/r)(\overline{C} - \overline{C}_w)dz + \pi R^2 W_n \overline{C} dz$$

$$\text{i.e. } u'dC'/dz = -(2D_{eff}/R^2 + W_n)\overline{C}$$

$$\overline{C} = C_o Exp(-k\tau)$$

Knowing experimental values of the change of concentration with time, it is possible to determine the effective turbulent velocity of reaction k and also the velocity of chemical reaction W_n.

EXPERIMENTAL RESULTS

The first test series has been carried out to investigate the effect of inlet fuel velocity on species and temperature profiles inside the combustor space without secondary air admission and at weak swirl conditions. A sample of the results is shown in Fig.3 with complete data in Ref.[18]. The results show that the radial temperature profiles posses two peaks specially at stations near to the burner exit. The central peak is due to the recirulated hot combustion products in the recirculation zone, while the outer peak appears where the main reaction zone begins in the turbulent mixing shear layer at fuel jet boundary. At downstream locations this peak is shifted towards the flame tube wall due to the spread of the fuel jet. The temperature profiles of the downstream positions are flattened and the temperture levels are higher. Figure 3 shows also that the radial carbon dioxide profile has two peaks at the same radial positions of temperature peaks. At further downstream positions these peaks tend to be more flat and CO levels generally increase. Regarding carbon monoxide and unburned hydrocarbon profiles both peaks exist in the fuel rich central zone and their levels decrease at downstream position in the combustor. However, as the flow velocity increases the unburned fuel and carban monoxide persist at further downstream positions in the combustor giving longer flame.

To study the effect of equivalence ratio on radial temperature and species profiles, the profiles measured at different equivalence ratios are compared at diffenent axial stations and a sample of these comparisons is shown in Fig.4. It is clear that lower temperature and carbon dioxide levels are observed at the lower equivalence ratios while opposite

trends are found for carbon monoxide and unburned hydrocarbons. However, the results show that at lower equivalince ratios the reacting flame is shorter and both carbon monoxide and unburned bydrocarbons disappear at shorter distances from the combustor exit.

The second testing series has been carried out to investigate the influence of secondary air admission on temperature and species distributions within the combustor. During this series of experiments both fuel and primary flow rates are kept constant to give a primary zone equivalence ratio of 1.0 while the secondary air flow rates have been varied to obtain an overall equivalence ratios of 0.45, 0.52 and 0.62. Figure 5 shows the contours of temperature, carbon dioxide and carbon monoxide at an equivalence ratio of 0.65. The comparison between these contours and those of Fig.6 which are obtained at same canditions but without secondary air admission, shows that the secondary air admission quenches the reaction of carbon monoxide near the wall at positions near to the combustor exit. On the other hand, at downstream locations, the secondary air penetrates the rich flame core and provides oxygen for CO oxidation resulting in low exhausted CO levels. However, at very low overall equivalence ratio the secondary air is observed to generally quench CO reaction even at the penetrated flame core due to the generally low temperatures of the combustion gases. Carbon dioxide levels drops near the wall at the positions near to the combustor exit and then through out the combustor at downstream positions due to the mixing effect of secondary air.

The temperature distribution along the combustor is significantly influenced by the addition of the secondary air. The maxinum temperature of 1900 to 2000°C, attained in the central primary reaction zone, drops significantly in the downstream positions due to the secondary air admission. Also the addition of the scondary air reduces the temperature of the regions near the wall and outside the main reaction zone. This would freeze the combustion in this zone and greatly affect CO and unburned hydrocarbon exhaust emissions. It is found also that the temperature gradients increases with the decrease of the overall equivalence ratio.

DISCUSSION AND ANALYSIS OF RESULTS

Local mole fractions of product species (X_i) have been calculated from the measured concentrations for CO_2, CO, O_2 and HC to obtain the local equivalence ratio, rate of oxygen consumption (X_{O_2}/X_{D_2O}) and the extent of reaction. A sample of these results is given in Fig.7 which shows the average oxygen consumption along the combustor at different overall equivalence ratios with and without secondary air admission. It is clear that without secondary air $O_2/O_{2,o}$

decreases more sharply in the primary reaction zone then remains constant or decreases slowly at the higher equivalence ratios. It is also noticed that the rate of decrease of the $O_2/O_{2,o}$ is higher for the higher equivalence ratios. In the case of the secondary air admission this ratio increases again at downstream positions in the combustor.

To determime the effective turbulent velocity of reaction, the previously mentioned analytical approach is adopted. The change of C/C_o with time has been calculated from the equivalence ratio contours for different fuel velocities and overall equivalence ratios. Drawing $\ln(\bar{C}/\bar{C}_o)$ versus time, a sample of which is given in Fig.8, it is possible not only to determine the effective velocity of turbulent reaction K but also the velocity of chemical reaction W_n for both the primary and secondary reaction zones. The constants K_v and K_ϕ of the effective velocity of turbulent reaction for natural gas-air mixtures are determined for the investigated range of operating conditions. A relation has been detected for the product $K_v.K_\phi$ in the following form:

$$K^2 = K_v.K_\phi = 800 + 254.5V_f\phi$$

Knowing that $K=[(0.08\ Re^{0.64})/d^2]+W_n$ and substituting for the turbulent reaction term, it is possible to determine the velocity of chemical reaction W_n in the following form

$$K^2_{W_n} = (K_v.K_\phi) = 500 + 200V_f\phi$$

The introduction of the secondary air increases K_ϕ to obout 1:4 times its value without secondary air and the values of K_ϕ are found to vary with the overall equivalence ratio according to the relations

for primary zone $K_\phi = 60 - 18.2\phi$
for secondery zone $K_\phi = 80 - 18.2\phi$

The velocity of the chemical reaction for the secondary zone has been determined and is found to be 79 s^{-1}. Moreover, the length of the combustion zone can be determined by the following formula.

$$L = (ud^2\ T/T_o) / (8D_{eff} + W_n d^2)$$

CONCLUSIONS

Species, temperature and velocity distributions are measured for a wide range of operting conditions for swirling reacting flow with and without secondary air admission. These data are used to define the turbulent velocity of combustion and the velocity of chemical reaction in the combustion and dilution zones. A generalized relation for the turbulent velocity of combustion has been deduced for different inlet fuel velocities and equivalence ratios in both zones. The

turbulent velocity of reaction increases with the increase of inlet fuel velocity and decreases with the increase of equivalence ratio. Moreover, a generalized relation for the effective viscosity has been deduced for different swirl ratios which gives a quite reasonable results when using K-ϵ model of turbulence in case of swirling confined flow. It is also found that the effective viscosity increases in the regions of large radial velocity gradients and reduces near the combustor wall. These data have to be determined also for liquid fuels.

REFERENCES

1- Heap,M.P., Lowes,T.M. and Walmsley,R.; Fourteenth Symposium (International) on Combustion, p.883,The Combustion Institute, 1973.

2- Mellor,A.M., Anderson,R.D., Altenkirch,R.A. and Tuttle,J.H.; Combust. sci Technol.,V6,p169,1972.

3- Bowman,C.T., Cohen,L.S., Spadaccini,L.J. and Owen,F.K.: Effects of Interaction Between Fluid Dyhamics and Chemistry on Pollutant Formation in Combustion, Paper presented at the stationary source combustion symp., Atlanta, GA, sept 1972.

4- Bowman,C.T. and Cohen,L.S.: Influence of Aerodynamic Phenomena on Pllutant Formation in Combustion, EPA Report 650/2-75-061a, 1975.

5- Spalding,D.B.: Proceeding of the symposium on emissions from continuous combustion systems (W. cornelius and W.G. Agrew, Eds) P.3, Plenum, 1972.

6- Swithenbank,J., Poll,I., Vincent,M.W. and Wright,D.D.: Fourteenth Symoposium International on Combustion, p 627, The combustion Institute, 1973.

7- Caretto,L.S. : Prog. Energy & Combust. sci, 1, 47, 1976.

8- Elghobashi,S.E and Abou-Arab,T.W.: Phys. Fluids, V 26, No 4, 1983.

9- Andrews,G.E. and Bradley,D.: Combust. & Flame, V 18, 133, 1972.

10- Andrews,G.E., Bradley,D., and Lwakabamba,S.B.: Fifteenth Symposium "International" on Combustion, p.622, The Combustion Intstitute, 1974.

11- Elkotb,M.M Bull. of the Faculty of Engineering, Cairo University, 1969.

12- Sawyer,R.F., TeixeiraD.P., snd Starkman,E.S.: J. Eng. For Power, ASME Trans. series A, Vol 91, No 4, P290, 1969.

13- Starkman,E.S., Mizutani,Y., Sawyer,R.F. and Teixeira,D.P.: The Role of Chemistry in Gas Turbine Emission; ASME Paper 70-GT-81, 1970.

14- Hori,M., Trans. Japan Sco., Mech. Engrs., V 37, No 295, p.566, 1971.

15- Owen,M.J., Gouldin,F.C., and Mclean,W.J.: Seventeenth Symposium "International" on Combustion, p.363, The Combustion Institute, 1978.

16- Vu,T.B. and Gouldint,F.C.: AIAA Journal, V 20, No.5, p.642, 1982.

17- Elkotb,M.M., Abou-Ellail,M.M., and Salem,S. : Rotating Flow and Nonisotropic Turbulence in Receprocating Engines, ASME, The Fluid Engineering Devision Ed. Teomon UzKan, 1982.

18- Mohmoud,M.M.: Effect of Turbulence on Secondary Combustion Products, M.SC. Thesis, Cairo University, 1984.

NOMENCLATURE

C	concentration, gm/m³
C_μ, C_D	turbulence model constants
d	diameter, m
D_t	diffusion coefficient, m³/s
k	kinetic energy of turbulence, m²/s²
$k_{\phi f}(C_f, C_o)$	source term in fuel diffusion equation, gm/m².s
$k_{\phi o}(C_f, C_o)$	source term in oxygen diffusion equation, gm/m².s
K	effective velocity of turbulent reaction, s^{-1},
K_v & K_ϕ	constant
l	length scale, m
L	length of combustion zone, m
r	coordinate
Re	Reynolds number
R	radius of combustor, m
T	temperature, K
u	axial velocity, m/s
v	radial velocity, m/s
W_r	velocity of chemical reaction, 1/s
x	coordinate
ϵ	dissipation rate of kinetic energy of turbulence, m³/s³
ρ	density, kg/m³
μ	dynamic viscosity, kg.m/s
σ_c	exchange coefficient
ν	kinematic viscosity, m²/s
ϕ	equivalent ratio
θ	coordinate
τ	time s

SUBSCRIPTS

eff	effective	f	fuel
o	oxygen, initial	t	turbulence
ϕ	equivalence ratio		

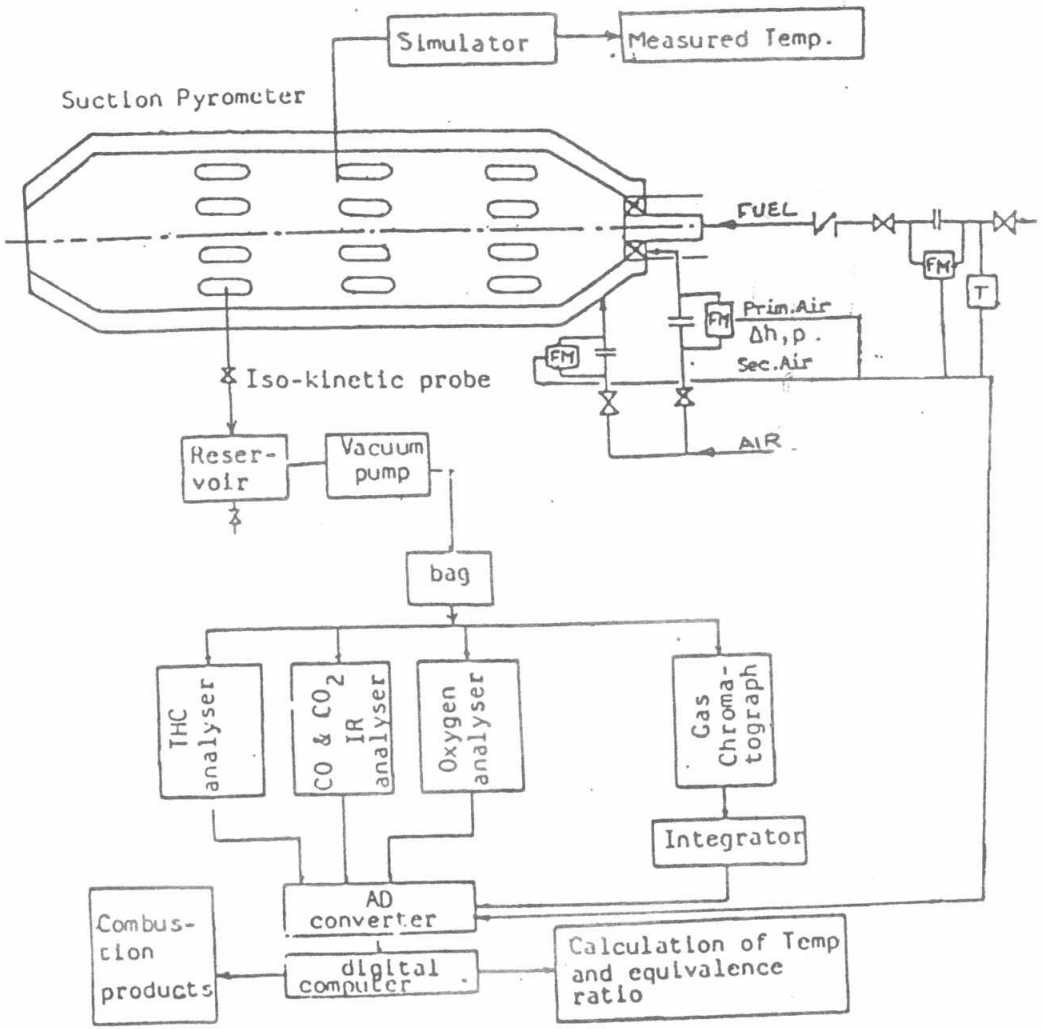

Fig.1. Schematic of the experimental setup

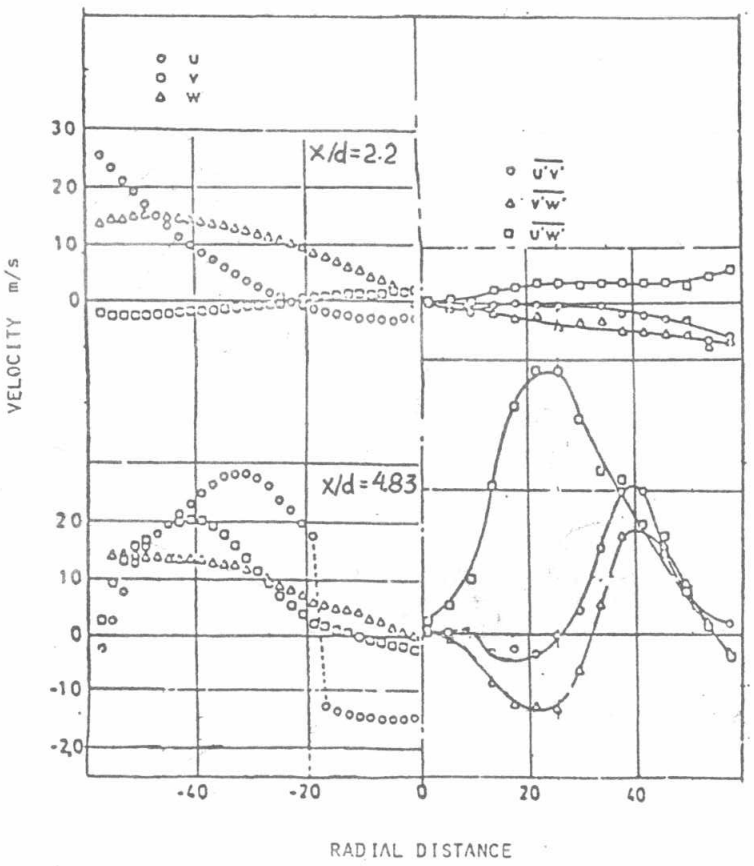

Fig.2. Radial distributions of mean and turbulent velocity components

SECOND A.S.A.T. CONFERENCE
21-23 April 1987, CAIRO

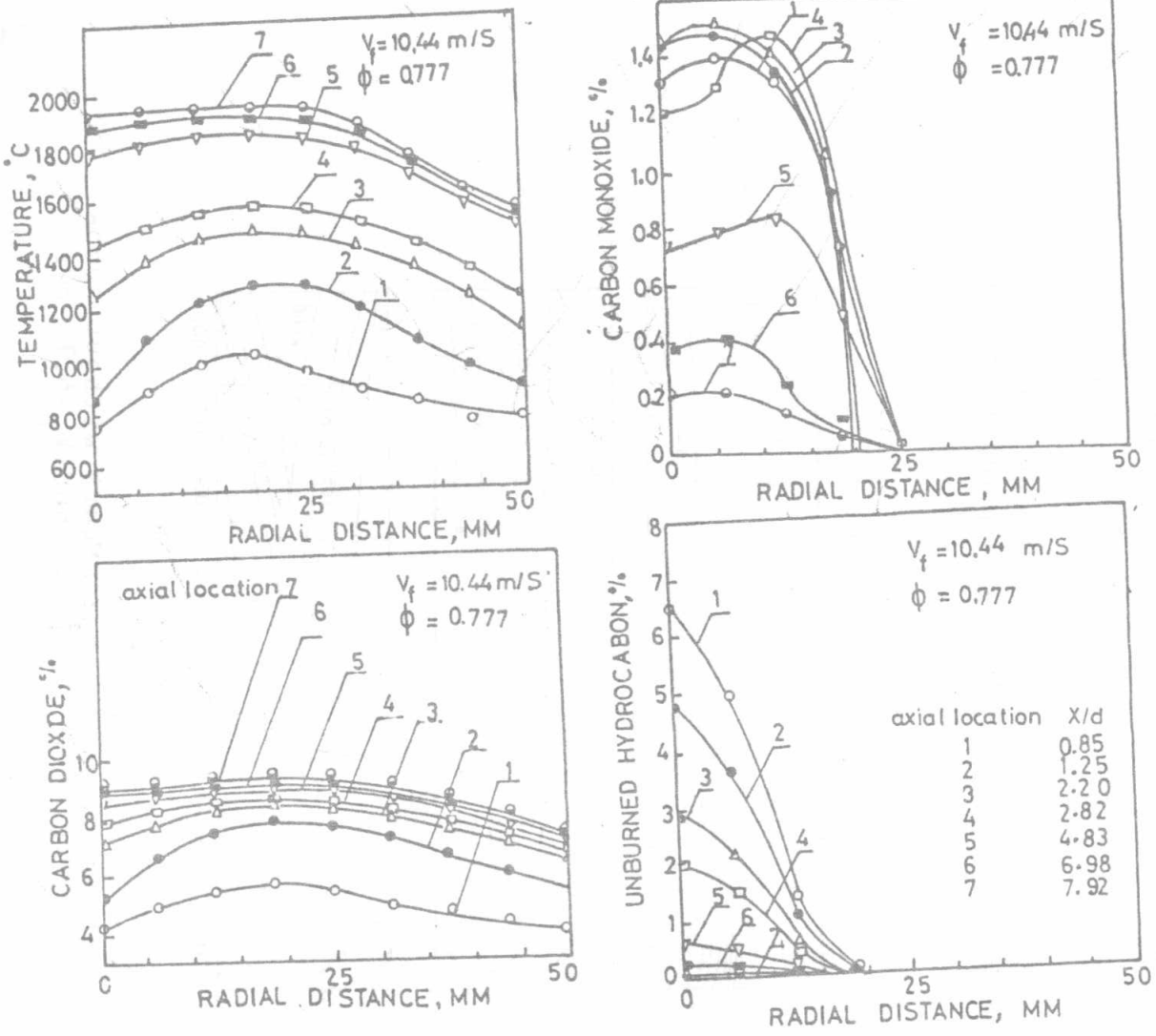

Fig.3. Radial profiles of temperature, CO_2, CO, and unburned hydrocarbons for V_f=10.44 m/s, ϕ=0.777 and without secondaty air addition.

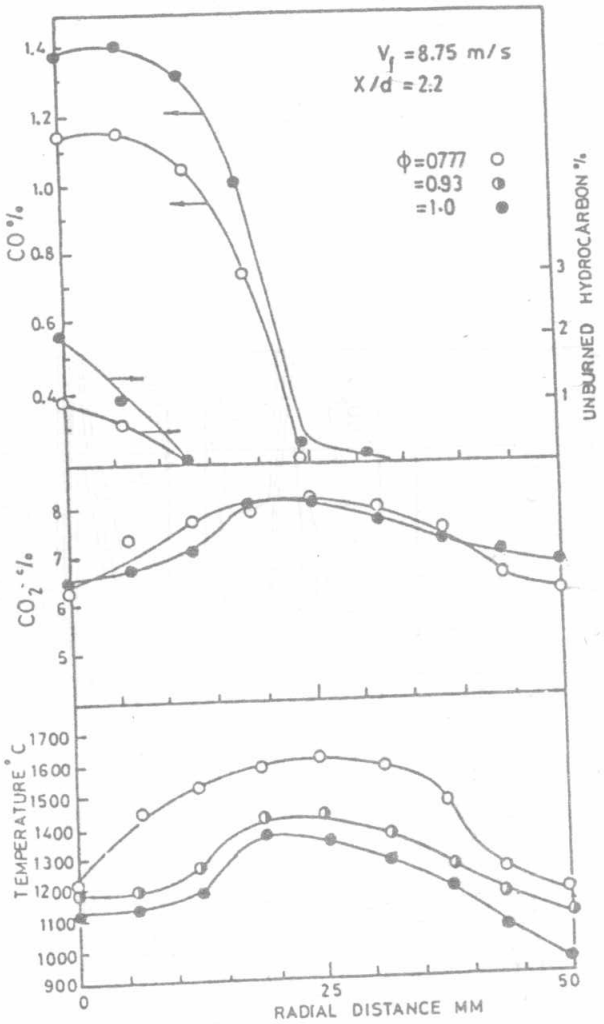

Fig.4. Effect of equivalence ratio on temperature and species profiles.

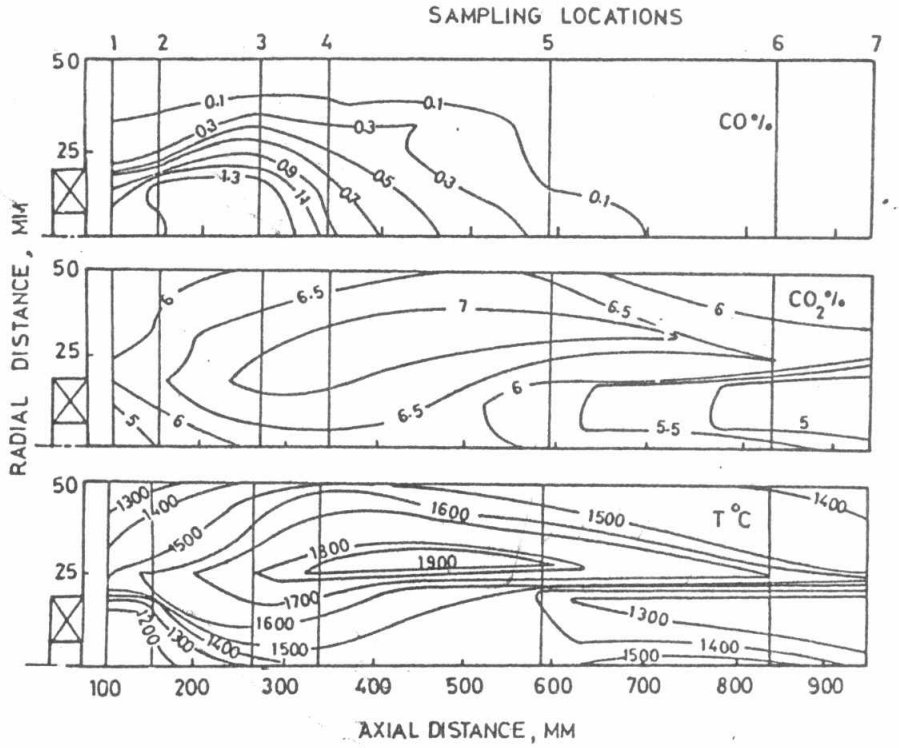

Fig.5. Temperature and species contours with secondary air addition for Φ=0.65aand V_f=6.16m/s.

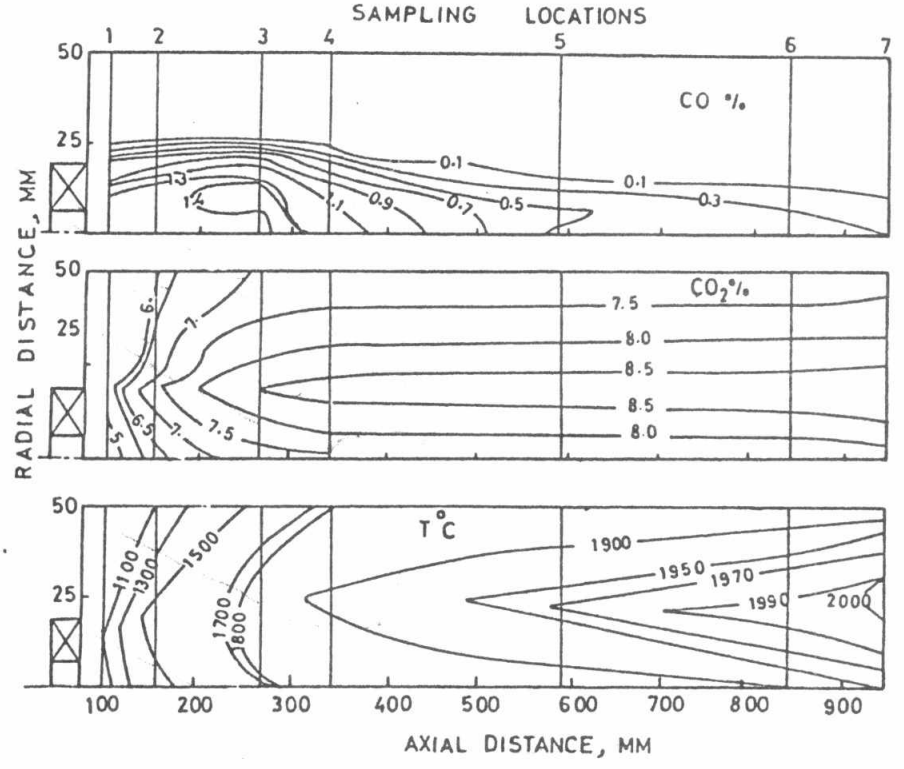

Fig.6. Temperature and species contours without secondary air addition for Φ=1.0 and V_f=6.16 m/s.

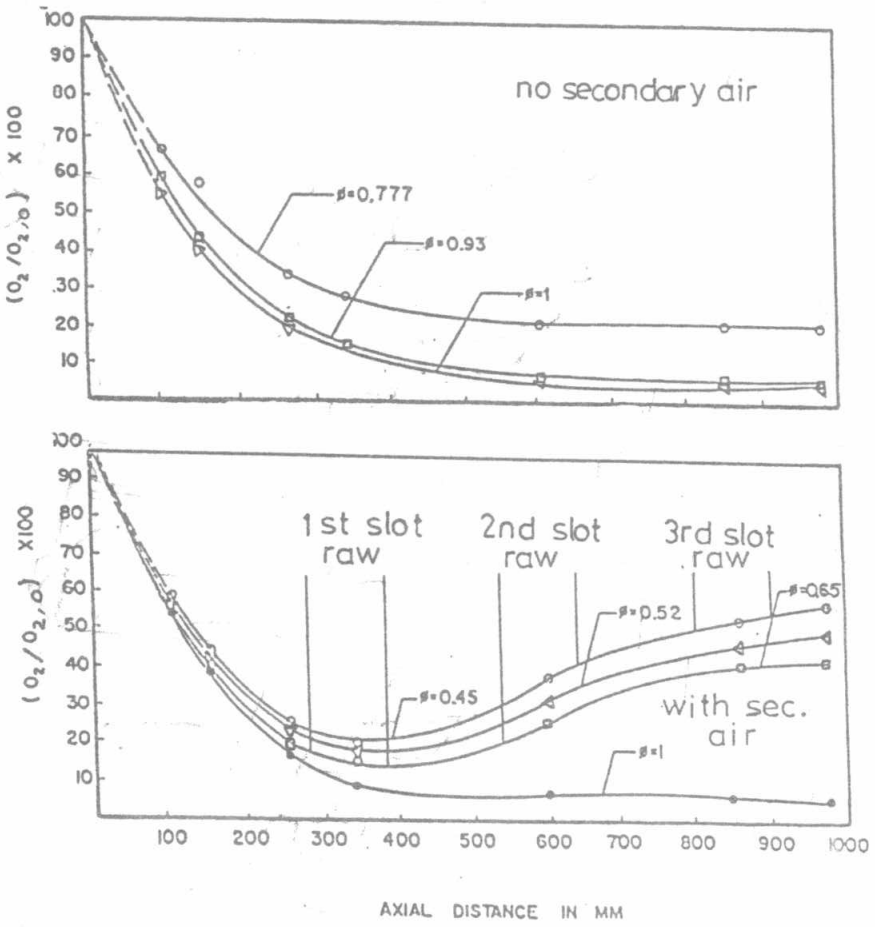

Fig.7. Variation of oxygen consumption along the combustor with and without secondary air addition.

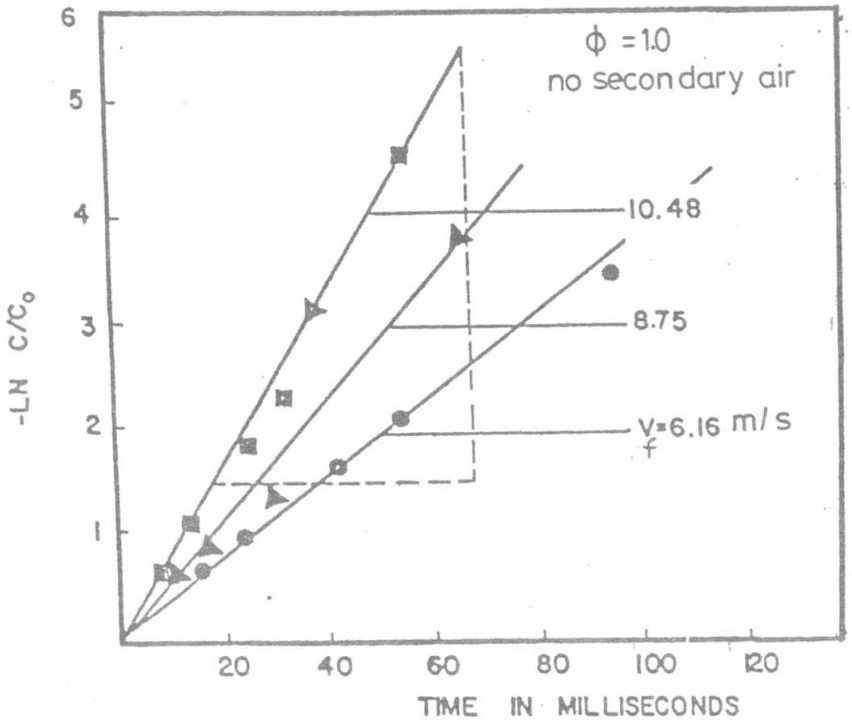

Fig.8. Variation of $\ln(C/C_o)$ with time for different fuel velocities.